

2022

## **Modular Data Center Direct Expansion HPAC Solutions – Application of R466A as Replacement for R410A**

Zvonimir Jankovic

Jaime Sieres

Branimir Pavkovic

Antun Barac

Follow this and additional works at: <https://docs.lib.purdue.edu/iracc>

---

Jankovic, Zvonimir; Sieres, Jaime; Pavkovic, Branimir; and Barac, Antun, "Modular Data Center Direct Expansion HPAC Solutions – Application of R466A as Replacement for R410A" (2022). *International Refrigeration and Air Conditioning Conference*. Paper 2342.  
<https://docs.lib.purdue.edu/iracc/2342>

This document has been made available through Purdue e-Pubs, a service of the Purdue University Libraries. Please contact [epubs@purdue.edu](mailto:epubs@purdue.edu) for additional information. Complete proceedings may be acquired in print and on CD-ROM directly from the Ray W. Herrick Laboratories at <https://engineering.purdue.edu/Herrick/Events/orderlit.html>

## Modular Data Center Direct Expansion HPAC Solutions – R466A as a Replacement for R410A

Zvonimir JANKOVIC<sup>1\*</sup>, Jaime SIERES<sup>3</sup>, Branimir PAVKOVIC<sup>2</sup>, Antun BARAC<sup>1</sup>

<sup>1</sup> Department of Energetics, Mechanical Engineering Faculty in Slavonski Brod, University of Slavonski Brod, Trg Ivane Brlić-Mažuranić 2, 35000 Slavonski Brod, Croatia  
zjankovic@unisb.hr

<sup>2</sup> Department of Thermodynamics and Energy Engineering, Faculty of Engineering, University of Rijeka, Vukovarska 58, 51000 Rijeka, Croatia  
branimir.pavkovic@riteh.hr

<sup>3</sup> Área de Máquinas y Motores Térmicos, Escuela de Ingeniería Industrial, University of Vigo, Campus Lagoas-Marcosende 9, 36310 Vigo, Spain  
jsieres@uvigo.es

\* Corresponding Author

### ABSTRACT

Direct expansion (DX) High Precision Air Conditioning (HPAC) cooling units for modular data centers operating with R410A are the focus of this article. The new potential long-term refrigerant R466A, as a replacement for R410A, for high density DX cooling units is analyzed. The steady state numerical model based on the test results of the R410A DX HPAC cooling unit is developed and validated for 5 steady state conditions. The model is used to simulate the unit HPAC DX to predict the thermodynamic conditions when the unit operates with R466A refrigerant, and the results were compared with R410A. The simulations were performed using the real boundary conditions to obtain results for the performance of the unit. The results show that the compressor produces between 11% and 14% higher refrigerant mass flow rates with R466A than with R410A. The EEV opening is between 2% and 5% higher with R466A than with R410A for the required superheat. Evaporating pressures are between 4.2% and 5.4% higher with R466A and condensing pressures are between 3.9% and 6.4% higher than with R410A. Cooling capacity and electrical power required for compressor work are higher for R410A than for R466A, a maximum of 4.5% and 8.1%, respectively. From a thermodynamic point of view, R466A is a very good substitute for R410A in data center cooling application.

### 1. INTRODUCTION

The modern lifestyle, work life, data storage, remote working, teaching platforms, etc. are enabled by an infrastructure called the Data Center; in other words: Infrastructure for our data storage and servers. The characteristics of data centers from the cooling point of view are:

- Almost all of the electrical energy consumed is eventually converted to heat;
- The cooling demand has a high density (high heat flux in a small area);
- Indirect cooling is used for data centers with a rated power greater than 150 kW (chillers with water or a suitable heat transfer fluid are used);
- Direct expansion cooling is used for modular data centers with a nominal power of up to 100 kW (special split systems DX are used);
- Approximately 50% of the price of the entire infrastructure is accounted for by the cooling system.

The focus of this article is on smaller capacity data center cooling or a dedicated DX system used primarily in smaller data centers. R410A refrigerant is the most common refrigerant in these split DX data center equipment due to its thermodynamic properties and small components. There is still no adequate alternative for R410A, but there are some options that are still under development and research. One good option is R466A, which is still questionable in terms of long-term solutions. However, from a thermodynamic point of view, it shows very good results as an alternative for R410A. The aim of this paper is to present the model and main results of R466A.

### 2. HIGH DENSITY DX HPAC COOLING UNIT FOR DATA CENTER

These devices are usually made in a split version. Units with compressor, evaporator and expansion valve are installed to cool the air in the room, while the condenser (usually air-cooled, with fans) is an outdoor unit. Such units

are often used to cool data centers, telephone base stations, and similar facilities with year-round cooling requirements. The cooling unit to be analyzed in this chapter is equipped with a scroll compressor and an electronic expansion valve. The condenser is not considered in this chapter, although the cooling unit was in operation during the experimental measurement along with the air microchannel condenser and only its measurement results are shown. However, the mathematical model of the condenser is described.

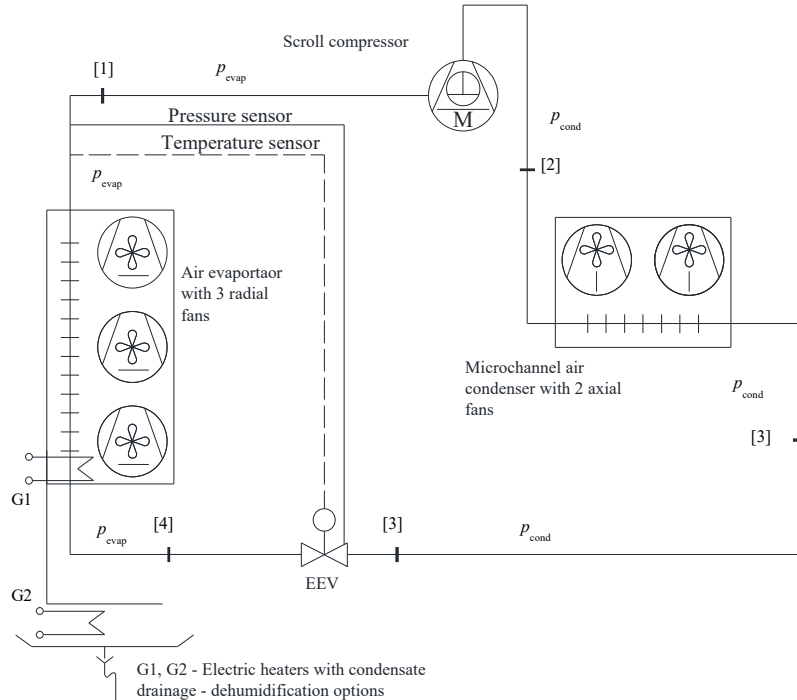


**Figure 1:** Schematic representation of air-to-air cooling unit (direct expansion)

The built-in scroll compressor is equipped with an inverter that theoretically delivers  $6 \text{ m}^3/\text{h}$  at 50 Hz or 2900 rpm. The inverter (frequency controller) regulates the speed from 1800 rpm up to 7200 rpm (frequencies from 30 to 120 Hz). The cooling capacity of the compressor ranges from 3.2 kW to 11.4 kW with an evaporating temperature of  $5^\circ\text{C}$  and a condensing temperature of  $50^\circ\text{C}$ , as well as a superheating of  $5^\circ\text{C}$  and a subcooling of  $4^\circ\text{C}$ . The electronic expansion valve has a nominal capacity of 13.7 kW for R410A refrigerant, with a condensing temperature of  $38^\circ\text{C}$  and an evaporating temperature of  $4^\circ\text{C}$  and a subcooling temperature of  $1^\circ\text{C}$ . The air evaporator is designed as a finned tube heat exchanger. The copper tubes are finned with smooth flat aluminum fins. The geometrical characteristics of the air evaporator for simulation are: Evaporator height  $H = 1500 \text{ mm}$ ; Evaporator length  $L = 400 \text{ mm}$ ; Length of tube in which refrigerant flows/evaporates  $L = 400 \text{ mm}$ ; Diameter of tube (inside/outside) in which refrigerant flows/evaporates  $d = 8/10 \text{ mm}$ ; Number of tubes  $N = 120$ ; Tubes are arranged in 2 rows; in the first row, to which the air flows, there are 59 tubes and in the second row there are 61 tubes; the number of evaporator sections is 8, with 5 tubes participating in each section, i.e. the total mass flow of the refrigerant is divided into 8 equal segments during the evaporation of the refrigerant; The distances between the tubes in depth and in height are equal, measured from center to center ( $F_D = 25 \text{ mm}$ ,  $F_H = 25 \text{ mm}$ ) and thus the distribution angles are  $60^\circ$ ; Fin spacing  $F_p = 1.75 \text{ mm}$ ; Number of fins 220; Fin thickness  $\delta_f = 0.1 \text{ mm}$ . The volumetric flow rate of air can range from 2800 to  $4000 \text{ m}^3/\text{h}$ . The air flow through the evaporator is made possible by 3 centrifugal fans. Condenser is air cooled microchannel with 2 axial fans. Mathematical model of condenser is not in the focus of this paper and it is not included.

### 3. MATHEMATICAL MODEL

For each component the mathematical model is developed. Simulation tool has been programmed using Engineering Equation Solver (EES, F-Chart) and the real boundary conditions were an input data (Table 5, without condensation temp.). All mathematical models take into account specific data and dimensions of components. The heat losses in refrigerant pipes are negligible; Pressure drops in the refrigerant pipes between main components are negligible.

### 3.1 Scroll compressor

The energy balance between the external part of the housing, the suction and discharge piping and the heat transfer between the cylinder, the electric motor and the lubricating and cooling oil inside the compressor is applied. The total balance also includes the electrical losses of the electric motor and the mechanical losses. The installed model allows predicting the temperature at the outlet of the compressor and the total power required to operate the scroll compressor.

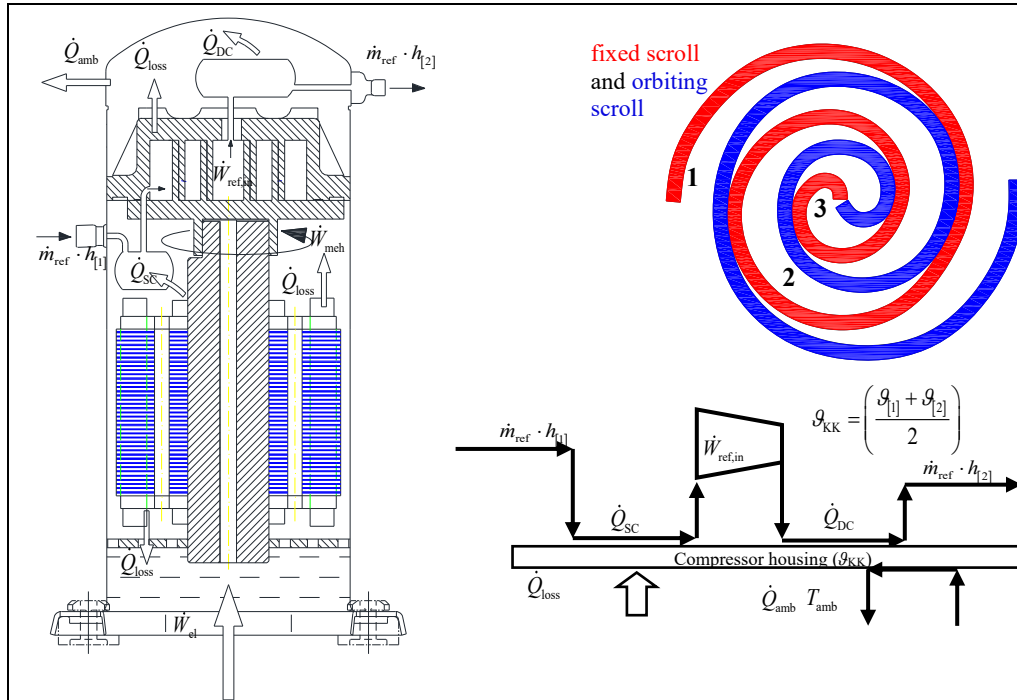


**Figure 2:** Schematic representation of scroll compressor mathematical model

The calculation of the mass flow of the refrigerant is modelled as an approximation to the isentropic process of compressing the working fluid between two scrolls, Fig. 2. The theoretical mass flow rate ( $\eta_{vol}=1$ ) is reduced by the mass flow rate that flows between the scrolls and generates volumetric losses; the following balance is established:

$$\frac{d\dot{m}_{ref}}{dt} = \frac{d\dot{m}_{ref(\eta_{vol}=1)}}{dt} - \frac{d\dot{m}_{ref(\Delta\eta_{vol})}}{dt} \quad (1)$$

In the volume between the fixed scroll and orbiting scroll marked with number 1, superheated vapor from the evaporator enters, in volume number 2 there is compressed vapor, while in volume 3 superheated vapor with condensation pressure exits. Losses occur due to the overflow of different states (1-2-3) between the contact lines of the two spirals, since the spirals cannot be perfectly sealed, which is taken into account in the model and the previous equation. Model of mass flow rate determination is described with correlations from Table 1 and 2.

**Table 1:** Correlations to calculate mass flow rate at ideal volumetric efficiency case

<p>To assume 100% compression of all the vapor whole vapor in the cylinder, the model is defined according to Wang (2008), and the expressions are:</p> $\frac{d\dot{m}_{ref(\eta_{vol}=1)}}{dt} = C_{RP} \cdot A_{comp} \cdot P_{[2]} \cdot \left\{ \frac{2 \cdot \kappa}{R \cdot (\kappa - 1) \cdot T_{[2]}} \cdot \left[ \left( \frac{P_{[1]}}{P_{[2]}} \right)^{\frac{2}{\kappa}} - \left( \frac{P_{[1]}}{P_{[2]}} \right)^{\frac{\kappa+1}{\kappa}} \right] \right\}^{\frac{1}{2}}$ <p>The approximation, based on the assumption of isentropic compression (isentropic exponent <math>\kappa</math>), is valid for the condition:</p> $\left( \frac{P_{[1]}}{P_{[2]}} \right) \geq \left( \frac{2}{\kappa + 1} \right)^{\frac{\kappa}{\kappa+1}},$ <p>while for the second condition <math>\left( \frac{P_{[1]}}{P_{[2]}} \right) &lt; \left( \frac{2}{\kappa + 1} \right)^{\frac{\kappa}{\kappa+1}}</math> the following approximation applies:</p> $\frac{d\dot{m}_{RT(\eta_{vol}=1)}}{dt} = C_{RP} \cdot A_{cyl} \cdot P_{[2]} \cdot \left\{ \frac{\kappa}{R \cdot T_{[2]}} \cdot \left[ \frac{2}{\kappa + 1} \right]^{\frac{\kappa+1}{\kappa-1}} \right\}^{\frac{1}{2}}$
--

The characteristics of the compressor and the influence of the oil and the refrigerant on the compression process are included in the flow (“correction”) factor for real gases  $C_{RP}$ . The value of this factor is determined experimentally Wang (2008). It can be very small, more precisely, have a greater impact, for example,  $C_{RP} = 0.1$ , as defined in the study Park (2002), or it can be determined that there is no impact,  $C_{RP} = 1$ , which is actually an ideal case (ideal gas). Studies Lee (2002) have compared these two values of flow factor (0.1 and 1) and concluded that for the assumed flow factor  $C_{RP} = 0.1$ , the agreement with experimental results is much better than in the case of  $C_{RP} = 1$ . The flow factor varies from case to case and from compressor to compressor. Based on the experimental results and monitoring the operation of the scroll compressor during this study is assumed to be in the interval:  $C_{RP} = 0.1 \dots 0.3$ .

**Table 2:** Correlations to calculate mass flow rate of overflow around spirals

<p>The part of the mass flow rate due to the overflow from the higher-pressure space to the lower pressure space between the walls of the scrolls or due to the impossibility of compressing all the aspirated refrigerant inside the cylinder space is defined by the following expression:</p> $\frac{dm_{RT(\Delta\eta_{vol})}}{dt} = C_{RP} \cdot A_{cyl} \cdot \left\{ \frac{\left[ 2 \cdot \left[ x_{vapor} \cdot \frac{\kappa}{\kappa-1} \right] \cdot \left( \frac{p_{[2]} - p_{[1]}}{\rho_{[2]} \rho_{[1]}} \right) + (1-x_{vapor}) \cdot \frac{p_{[2]} - p_{[1]}}{\rho_{liquid}} \right]^{\frac{1}{2}}}{\frac{x_{vapor}}{\rho_{[1]}} + \frac{(1-x_{vapor})}{\rho_{liquid}}} \right\}$ <p>The above expression can also be applied to the simulation of liquid injection into the compressor, as defined in Wang (2008).</p>	
---	--

Using the presented model to calculate the mass flows of the refrigerant even allows calculating the volumetric efficiency of the scroll compressor:

$$\eta_{vol} = 1 - \left( \frac{dm_{RT(\Delta\eta_{vol})}}{dt} \bigg/ \frac{dm_{RT(\eta_{vol}=1)}}{dt} \right) \tag{2}$$

The energy balance of the compressor, explained more detail in the paper Byrne (2014), is defined by the following expression based on the described approximation:

$$\dot{Q}_{loss} + \dot{Q}_{DC} = \dot{Q}_{amb} + \dot{Q}_{SC} \tag{3}$$

The heat flux generated by cooling the interior of the compressor is already known and is divided into the heat flux rates of mechanical and electrical losses, and finally, the already known derived expression:

$$\dot{Q}_{loss} = \dot{Q}_{loss,mech} + \dot{Q}_{loss,el} \rightarrow \dot{Q}_{loss} = \dot{W}_{el} \cdot (1 - \eta_{el} \cdot \eta_{mech}) \tag{4}$$

Total electrical input power for the compressor drive is equal to the enthalpy difference between the input and output state of the refrigerant from the compressor, increased by the amount of heat released to the environment:

$$\dot{W}_{el} = \dot{m}_{ref} \cdot (h_{[2]} - h_{[1]}) + \dot{Q}_{amb} \tag{5}$$

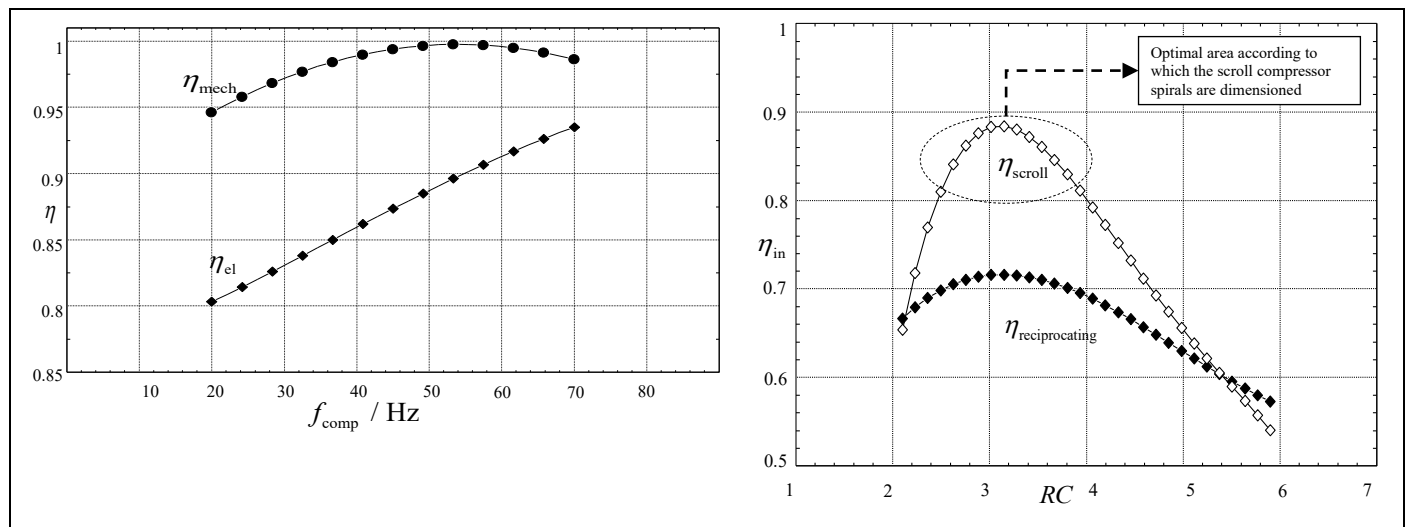


**Figure 3:** Diagram of electrical and mechanical efficiency of scroll compressor and indicated efficiency of scroll compressor compared to indicated efficiency of reciprocating compressors

The efficiency  $\eta_{el}$  of electric motor and the mechanical losses, i.e. the mechanical efficiency  $\eta_{mech}$  for the group of scroll compressors are defined by correlations according to the paper Park (2002). Both efficiencies are only a function of the operating frequency of the compressor's electric motor  $f_{comp}$ , and the correlation for the mechanical efficiency takes into account the friction between the scrolls. Both functions are shown on the previous figure, together the indicated efficiency of scroll and reciprocating compressors simulated in this work to show the difference in the tendency of the two functions. Assuming that the reciprocating compressor has better or closer indicated efficiency than the scroll compressor (which could be the case), scroll compressors have better indicated efficiency only for the narrow range of compression ratios for which they are designed.

The heat flux that the compressor gives off to the environment,  $\dot{Q}_{amb}$ , is defined by the total thermal conductance of the compressor housing  $(k \cdot A)_{KK}$  according to and the expression is

$$\dot{Q}_{amb} = (A \cdot k)_{KK} \cdot (T_{KK} - T_{amb}) \quad (6)$$

Coefficient  $(k \cdot A)_{KK}$  in W/m<sup>2</sup>K is defined based of the experimental reference states defined in the paper Byrne (2014).

### 3.2 Electronic expansion valve

The mathematical model of the electronic expansion valve (EEV) was developed to be used for various vapour compression applications and cooling capacities. The EEV increases or decreases its orifice area to allow a refrigerant mass flow that provides the best use of the evaporator heat exchange area required to maintain the required refrigerant superheat.

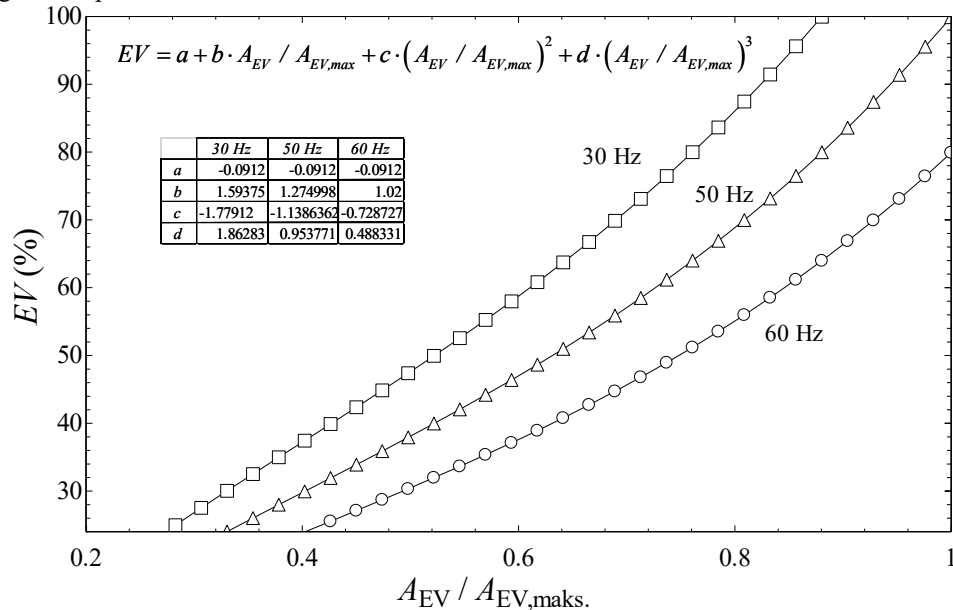


**Figure 4:** Correlation of EV opening in the function of the ratio of required and maximal flow area

The models of all parts of the refrigeration unit use the refrigerant mass flow rate defined by the compressor model that must converge through the expansion valve, resulting in the required flow area and percentage of expansion valve opening required, which provides information on the required valve capacity and valve opening. Based on this, dimensionless correlations were developed to calculate the valve opening as a function of the ratio between the actual flow area  $A_{EV}$  and the maximum flow area  $A_{EV,max}$ , of the valve. The dimensionless correlations are shown in the diagram of next figure for different operating frequencies of the compressor or different refrigerant mass flow rates. The same correlations may be used for EEV and standard mechanical expansion valves (EV).

To calculate the mass flow through the expansion valve, we need to calculate the flow factor  $C_{EV}$ , the flow area  $A_{EV}$ , the expansion factor  $Y_{EV}$ , the density of the liquid phase of the refrigerant  $\rho_{[3]}$  at the inlet of the expansion valve, and the pressure difference that the valve must relieve  $\Delta p_{EV}$ :

$$\dot{m}_{ref} = C_{EV} \cdot A_{EV} \cdot Y_{EV} \cdot \sqrt{(2 \cdot \rho_{[3]} \cdot \Delta p_{EV})} \quad (7)$$

The expansion factor  $Y_{EV}$  includes the change in refrigerant density flowing from the valve inlet to the inlet in the area of reduced pressure, related to the change in flow area as well as the pressure drop across the valve (Table 3). The expansion factor is influenced by the ratio between the diameters of the needle and the valve opening, the ratio of the pressure drops, the ratio of the specific heat capacities and the flow characteristics.

**Table 3:** Correlations for expansion factor calculation (American National Standards Institute, 2007)

$Y_{EV} = 1 - \frac{x_{EV}}{3 \cdot F_k \cdot x_T}; F_k = \frac{\left(\frac{c_p}{c_v}\right)}{1,4}$	
$x_{EV} = \frac{\Delta p_{EV}}{p_{[3]}} = \frac{P_{cond} - P_{evap}}{p_{[3]}}; x_{EV} = F_k \cdot x_T \rightarrow \text{"choked flow"} (Y_{EV} = 2/3)$	
$x_{EV}$	pressure differential ratio of expansion valve
$x_T$	pressure differential ratio for heat influence of fluid (in this case R290)

Calculation of the flow factor is based on Buckingham  $\pi$ -theorem W. Li (2013). Flow factor  $C_{EV}$  is in the function of subcooling temperature and valve opening.

$$C_{EV} = e_1 \cdot \pi_1^{e_2} \cdot \pi_2^{e_3} \quad (8)$$

where  $\pi_1$  defines the valve opening, and  $\pi_2$  presents relation between superheat degree and critical temperature of refrigerant as follows:

$$\pi_2 = \Delta g_{sub} / g_{ref,critical} \quad (9)$$

The geometry input data of EV is based on the research papers of W. Li (2013), Y. Qifang (2007) and Z. Chuan (2006), while empirical coefficients for calculating the flow factor were determined experimentally in the named researches.

The idea of the described approach in modelling the EEV or standard EV is to allow the application of the model to the different refrigeration units with similar expansion valves and different performances.

### 3.3 Air evaporator

The heat transfer coefficient on the air side is modeled for sensible and latent heat. Air cooling evaporators can be modeled for sensible heat only, but it is also important to consider the dew of moisture from the air on the surface of the fins and tubes (latent heat). The balance applies to all air-cooling evaporators:

$$\dot{Q}_{evap} = \dot{Q}_{evap,air} = \dot{Q}_{air,sensible} + \dot{Q}_{air,latent} \quad (10)$$

Exchanged sensible heat of air in the evaporator:

$$\dot{Q}_{air,sensible} = \dot{m}_{evap,air} \cdot c_{p,air} \cdot (g_{evap,air,inlet} - g_{evap,air,outlet}) \quad (11)$$

Latent heat:

$$\dot{Q}_{air,latent} = \dot{m}_{w-\Delta x} \cdot (h_{air+H_2O,inlet} - h_{air+H_2O,outlet}) \quad (12)$$

The heat transfer coefficient of the evaporation of the refrigerant in two-phase flow in horizontal tubes was calculated by modified correlations of Chen (2014), where the heat transfer coefficient was calculated in the single-phase part of the refrigerant according to the Dittus-Boelter (1985) correlation and bubble evaporation was calculated according to the Copper (1984) correlation for evaporation in tubes, the expression is as follows:

$$\alpha_{nb} = 55 \cdot p_{evap} / p_{cr} \cdot \left( -\log(p_{evap} / p_{cr}) \right)^{-0,55} \cdot M_{mol,ref}^{-0,5} \cdot q_{nb}^{0,67} \quad (13)$$

The heat transfer coefficient on the air side  $\alpha_{air}$  is calculated according to the correlation of the Colburn  $j$ -factor, Chilton and Colburn (1934), for dry fin surfaces following Wang (2000), where the detail model can be followed. Using the known  $j$ -factor as a dimensionless number, the airside heat transfer coefficient  $\alpha_{air}$  for the airflow between the fins, defined for the free surface for the airflow  $A_{air,free}$ , is calculated according to the expression:

$$\alpha_{air} = \frac{j_{air} \cdot c_{p,air} \cdot \dot{m}_{air}}{A_{air-free} \cdot (Pr_{air})^{(2/3)}} \quad (14)$$

The mass transfer model is simplified by the following assumptions: one-dimensional flow, homogeneous temperature of moist air, and equal heat transfer coefficient around all tubes within a control volume or exchange area. The model is described for one control volume, but in modeling, if the exact geometry of the heat exchanger (air evaporator or cooler) is known, it can be assumed that the entire heat exchanger is exactly one control volume.

The developed model is described following Lienhard (2008). The mass flow rate of water due to dew formation on the outer surface (tube wall) of the heat exchanger is calculated from the following expression:

$$\dot{m}_{w-\Delta x} = -\Delta A_{w-\Delta x} \cdot B_{m-\Delta x} \cdot g_{m-\Delta x} \cdot \quad (15)$$

Correlations to include this equation into mathematical model are given in the next table.

**Table 4:** Correlations for mass transfer calculation in the air side of evaporator

The driving force of mass transfer $B_{m-\Delta x}$ is calculated for a two-component mixture of water vapor and dry air according to the expression: $B_{m-\Delta x} = \frac{\zeta_{A,0} - \zeta_{A,S}}{\zeta_{A,S} - 1}$
The mass transfer coefficient is: $g_{m-\Delta x} = \left( \frac{Sh_{air-\Delta x} \cdot \rho_{VP} \cdot D_{m,VP}}{d_{hyd}} \right) \cdot \left( \frac{\ln(1 + B_{m-\Delta x})}{B_{m-\Delta x}} \right)$
The mass diffusivity of water vapor $D_{m,VP}$ through the air, its empirical correlation: $D_{m,VP} = 1,87 \cdot 10^{-10} \cdot \left( \frac{T_{air}^{2,072}}{P} \right)$ <i>(From the correlation, calculated mass diffusivity in m<sup>2</sup>/s by including the temperature in Kelvin and the pressure in atmospheres. (1 atm = 101325 Pa)</i>
The Schmidt number (Sc) is the ratio between the kinematic viscosity ( $\mu$ ) of air and the mass diffusivity of water vapor: $Sc_{air-\Delta x} = \frac{\mu_{air}}{D_{m,VP}}$

The values of  $B_{m-\Delta x}$  are negative along the entire length of the heat exchanger, which is due to the fact that the mass fraction of moisture along the cold wall  $\zeta_{A,S}$  is less than the mass fraction of moisture away from the wall  $\zeta_{A,0}$  for each control volume (heat exchanger). Due to the described difference in the mass fractions of moisture, dew formation occurs along the entire length of the exchanger (control volume). The absolute value of the driving force of mass transfer is highest at the air inlet of the heat exchanger because the mass fraction of moisture in the air is highest at the inlet and decreases with length/depth due to dewing, so the difference in moisture content is greatest in this part and decreases as the length/depth of the heat exchanger increases. During dew formation, the moisture content of the moist air is higher than the moisture content directly on the wall, so the driving force of mass transfer is negative. Based on the described the minus sign in equation (15) is present to calculate water condensation mass flow rate  $\dot{m}_{w-\Delta x}$  where  $g_{m-\Delta x}$  is mass transfer coefficient and  $\Delta A_{m-\Delta x}$  is the exchange surface for dew of moisture.

#### 4. TESTING OF THE HPAC DX UNIT AND MODEL VALIDATION

The cooling device tested was designed for data center cooling. The tests performed were complex and included a large number of parameters, of which the data related to the cooling of the air in the room will be presented here. During the test, two cooling units were set to cool the air to a temperature of 35°C and a relative humidity of 35% to a dry bulb temperature of 23 ± 1°C and a relative humidity of 55% ± 5%. This unit uses R410A as the working fluid and belongs to the group of direct expansion cooling units. Testing results are presented in the following table.

**Table 5:** Data from experimental procedure of a direct expansion cooling unit

Test	Rpm, min <sup>-1</sup>	Compressor frequency, Hz	Condensation temperature, °C	Evaporator volume flow rate, m <sup>3</sup> /h	Air temperature at the inlet of the evaporator, °C	Relative humidity at the inlet of the evaporator, %
1	5672	94.5	43.92	3999	32.2	33
2	5582	93	44.41	3882	34.3	34
3	5625	93.8	44.35	3863	34.3	32
4	5575	92.9	44.1	3297	34.2	33
5	5528	92.5	44.51	3530	35.4	34
6	5412	91.1	44.03	2824	35.2	34

The cooling unit belongs to the group of "HPAC" ("High Precision Air Conditioning") units, which means that they are cooling units that have high precision and the ability to quickly regulate the operation and self-protection under various conditions 365 days a year, 24 hours a day. The design and components of the cooling unit have already been described. During the data center test, the air conditioning system was tested and 3 uniform operating cases were digitally recorded for each cooling unit, for a total of 6 uniform cases. On the next photo flop plan of the data center and measuring is presented; here is only focus on the HPAC unit; the air temperature was measured at the inlet and outlet of the cooling unit to confirm steady state (type K thermocouples 10 points on the photo).

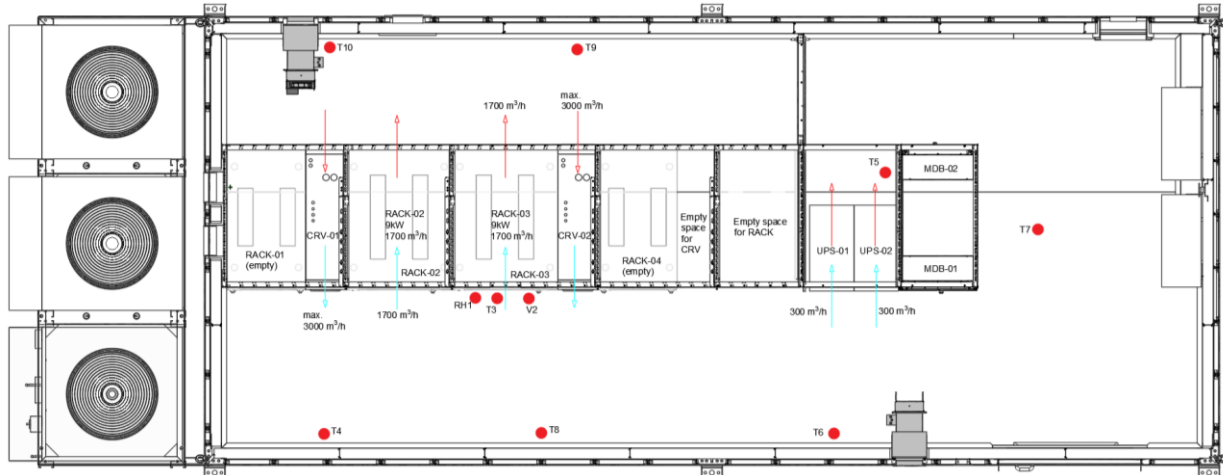


**Figure 6:** Data Center temperature and air circulation testing (cooling)

#### 4.1 Evaluation of the mathematical model

In this work, a numerical model was developed for the simulation of the described specialized cooling unit for the cooling of computer/server's equipment. The following table shows the results of the evaluation of the developed mathematical model in comparison with the measured values. Comparison includes models of the scroll compressor, EEV and air evaporator with the humidity model. The simulation results of the cooling unit compared to the experimental results are shown in the following 3 tables. The results confirm the reliability of the model, results of simulations are very close to the experimental (measured) values.

**Table 6:** Comparison of results: evaporation temperatures and compressor outlet temperatures

TEST	Evaporation temperature, °C		Compressor outlet temperatures RT, °C	
	<i>Exp.</i>	<i>Sim.</i>	<i>Exp.</i>	<i>Sim.</i>
1	8.42	9.641	75.59	70.56
2	9.58	8.734	72.9	69.64
3	8.87	8.759	73.81	70.17
4	9.07	8.712	74.25	70.81
5	10.08	12.95	75.96	72.95
6	6.02	6.138	76.9	71.28

**Table 8:** Comparison of the state of cooled air at the outlet of the cooling unit (evaporator)

TEST	Air temperature at the outlet of the unit, °C		Relative humidity, %	
	<i>Exp.</i>	<i>Sim.</i>	<i>Exp.</i>	<i>Sim.</i>
1	22.9	22.9	0.5685	0.5685
2	24.6	24.42	0.5948	0.6011
3	24.7	24.55	0.5565	0.5615
4	22.9	22.82	0.636	0.639
5	24.3	24.64	0.6436	0.6308
6	23.6	23.48	0.6639	0.6688

**Table 7:** Comparison of results: mass flow rates, heat flow rates in the evaporator and opening of EEV

TEST	Mass flow rate RT, kg/h		Heat flow rate in the evaporator, kW		Opening EEV-a, %	
	<i>Exp.</i>	<i>Sim.</i>	<i>Exp.</i>	<i>Sim.</i>	<i>Exp.</i>	<i>Sim.</i>
1	264.5	266	12.3	12.3	77.66	70.85
2	269.9	273.8	12.4	12.63	75	70.89
3	264.9	269	12.2	12.4	73.77	70.15
4	264.4	265.8	12.3	12.39	73.77	70.46
5	272	267.1	12.9	12.5	75.61	73.15
6	231.4	234	10.8	10.91	57.37	63.14

## 5. SIMULATION RESULTS

A good potential substitute that has recently appeared on the market is the working fluid R466A (GWP=733), whose safety class is A1 and B1, i.e., it is neither toxic nor flammable. Since no detailed data on the efficiency of the refrigeration system for this refrigerant (R466A) has been found in the literature so far, simulations have been carried out and the results are presented below.

Simulation of HPAC unit is provided with air temperature at the inlet of the evaporator is varied from 30 to 40°C; degree of superheat 7°C defined by the operation of the EEV; air temperature at the inlet of the condenser is 35°C;

The air flow rate in the evaporator is 11000 m<sup>3</sup>/h and in the condenser 23000 m<sup>3</sup>/h. The operating frequency of the compressor is 50Hz, which gives a capacity of 17 m<sup>3</sup>/h (*real boundary conditions*).

The simulation of the operation of the refrigeration unit shows that the mass flow rate is 11 to 14% higher with the working fluid R466A compared to R410A, Figure 7. The increase in the opening of the expansion valve is in the range of 2 to 5% for the working fluid R466A compared to the working fluid R410A to maintain the desired superheat of 7°C. Figure 8, shows the temperatures of the two working fluids (R466A / R410A) at high and low pressure. It can be seen that the evaporating temperatures are within ± 0.69°C and the condensing temperatures are practically the same (± 0.15°C). The temperatures of the R466A working fluid after compression are on average (arithmetic mean) 6.6°C higher than those of the R410A working fluid under the same real boundary conditions.

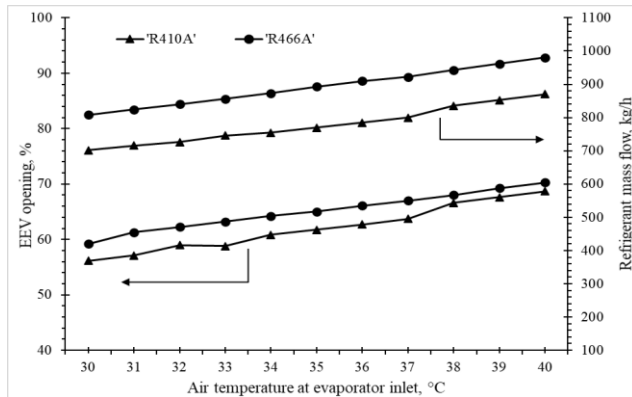


Figure 7: Comparison of opening of EEV-a and mass flow rates R410A/R466A

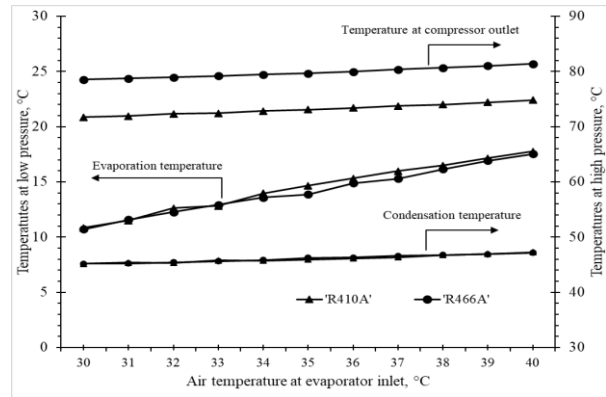


Figure 8: Comparison of working fluids temperatures R410A and R466A

Based on the presented values in the previous graphs it can be observed; The condensing pressures for the R466A working fluid are 3.9% to 6.4% higher than the pressures for the R410A working fluid, while the evaporating pressures for R466A are 4.2% to 5.4% higher than the evaporating pressures for R410A. Ultimately, the pressure ratios for both working fluids give the same compression ratios, which are slightly (1.5 to 2.3%) higher for the R410A working fluid. The heat flux in the evaporator is higher by a maximum of 4.5% for R410A compared to R466A. To drive the compressor, you need to invest a maximum of 8.1% more current to compress the R466A working fluid than for R410A, which ultimately results in a higher COP for R410A of a maximum of 7.4% compared to R466A.

## 6. CONCLUSIONS

The methodology and validity of the models developed in this research for the cooling unit were confirmed. For the operation of refrigeration units in air conditioning systems with direct expansion, the working fluid R410A is very often used. It is a much more interesting working fluid when it comes to researching an appropriate replacement, since its high pressures and densities allow minimization of refrigerant components and there is almost no possibility of replacement without using flammable refrigerants such as R32. Recently, blends of R32 and R125 have been studied with substances that reduce the flammability of the blend (such as CF3I)... The researches on this topic is ongoing today in the world's industry.

Based on this paper research; It can be said that the refrigerant R466A as refrigerant replacement shows very good thermodynamic match; for the long term use the refrigerant is questionable in compatibility with some materials, based on the feedback from industry.

## NOMENCLATURE

\*All subscript numbers in angle brackets (e.g. [1]) in mathematical model follows same numbers at Figure 1.

\*In the nomenclature are included only main variables, rest of variables are covered in the paper.

$A$	surface	m <sup>2</sup>
$c_p / c_v$	Specific heat capacity ( <i>constant pressure, constant volume</i> )	J·kg <sup>-1</sup> ·K <sup>-1</sup>
$d$	diameter	m
$h$	Specific enthalpy	J·kg <sup>-1</sup>
$\dot{m}$	mass flow rate	kg·s <sup>-1</sup>
$\dot{m}_{m-\Delta x}$	flow rate of water due to dew formation/condensation	kg·s <sup>-1</sup>
$M_{mol}$	Molar mass	kg·kmol <sup>-1</sup>

$p$	Pressure	Pa
$\dot{Q}$	Heat flux	W
$t$	time	s
$T$	Temperature	K
$\dot{W}$	Power	W
$x$	Quantity	kg·kg <sup>-1</sup>
$\rho$	Density	kg·m <sup>-3</sup>
$\eta$	Efficiency	-
$\alpha$	Heat transfer coefficient	W·m <sup>-2</sup> ·K <sup>-1</sup>
$\vartheta$	Temperature	°C
$\Delta$	Difference or loss	J·kg <sup>-1</sup>

**Subscript**

amb	ambient	cyl	cylinder
cond	condenser/condensation	cr	critical
DC	suction chamber	evap	evaporator/evaporation
hyd	hydraulic	in	indicated
nb	nucleate boiling	ref	refrigerant
vol	volumetric	VP	water vapor (from air)
SC	suction chamber		
m- $\Delta x$	mass change by changing the air quantity		
w- $\Delta x$	water change by changing the air quantity		

**REFERENCES**

- American National Standards Institute (2007). ISA-75.01.01-2007 (60534-2-1 Mod): Flow Equations for Sizing Control Valves, *Research Triangle Park*, North Carolina 27709, USA: American National Standards Institute
- Byrne P., R. Ghouali and J. Miriel (2014). Scroll compressor modelling for heat pumps using hydrocarbons as refrigerants. *International Journal of Refrigeration*
- Chen G. F., M. Q. Gong, S. Wang, J. F. Wu i X. Zou (2014), »New flow boiling heat transfer model for hydrocarbons evaporating inside horizontal tubes« u American Institute of Physics, AIP Conference Proceedings 1573 (1092), Anchorage, Alaska, USA
- Chilton T. i A. Colburn (1934), Mass transfer (absorption) coefficients prediction from data on heat transfer and fluid friction *Ind. Eng Chem, 26*
- Lienhard IV John H. (2008), A Heat Transfer Textbook, 3rd edition, SAD: Phlogiston Press
- Cooper M. (1984) Heat flows rates in saturated pool boiling – A wide ranging examination using reduced properties *Adv. Heat Transf. 16, p. 157–239*
- Chuan Z., Shanwei M., Jiangpin C., and Zhijiu C. (2006.), Experimental analysis of R22 and R407c flow through electronic expansion valve, *Energy Conversion and Management 47, p. 529–544*
- Dittus P. and Boelter L. (1985). Heat transfer in automobile radiators of the tubular type. *Int. Commun. Heat Mass Transfer pp. 3-22, 12*
- Lee B. C., T. Yanagisawa, M. Fukuta i S. Choi, (2002) »A Study On The Leakage Characteristics Of Tip Seal Mechanism In The Scroll Compressor Purdue International Compressor Engineering Conference. Paper 1586
- Li W. (2013) Simplified modeling analysis of mass flow characteristics in electronic expansion valve *Applied Thermal Engineering 53, pp. 8-12*
- Qifang Y., Jiangping C. and Zhijiu C. (2007) Experimental investigation of R407C and R410A flow through electronic expansion valve *Energy Conversion and Management 48, pp. 1624-1630*
- Park Y. C., Y. Kim i H. Cho (2002), »Thermodynamic analysis on the performance of a variable speed scroll compressor with refrigerant injection« *International Journal of Refrigeration 25 p. 1072–1082*
- Wang B., W. Shi, X. Li i Q. Yan (2008), »Numerical research on the scroll compressor with refrigeration injection« *Applied Thermal Engineering 28, p. 440–449*

**ACKNOWLEDGEMENT**

This research was in part funded by University of Rijeka project (uniri-tehnic-18-14). Thanks also go to the company Vertiv from Croatia, manufacturer of data centers, and Vertiv from Italy, manufacturers of the DX HPAC devices, who provided us with all the technical information for the research.